Piezoelectric response of charged non-180° domain walls in ferroelectric ceramics

Zhanfang Li, Hao Wu, and Wenwu Cao

Citation: J. Appl. Phys. **111**, 024106 (2012); doi: 10.1063/1.3679084
View online: http://dx.doi.org/10.1063/1.3679084
View Table of Contents: http://jap.aip.org/resource/1/JAPIAU/v111/i2
Published by the American Institute of Physics.

Piezoelectric response of charged non-180° domain walls in ferroelectric ceramics

Zhanfang Li,[1] Hao Wu,[1] and Wenwu Cao[1,2,a)]
[1]*Condensed Matter Science and Technology Institute, Harbin Institute of Technology, Harbin 150001, China*
[2]*Materials Research Institute, The Pennsylvania State University, University Park, Pennsylvania 16802, USA*

(Received 19 August 2011; accepted 29 December 2011; published online 26 January 2012)

Charged domain walls may have lower energy than charge neutral walls when large amount of aliovalent doping are present or when there are substantial amount of charged defects in the system. Charged domain walls can produce much larger contribution to functional properties than charge neutral domain walls because they are energetically less stable. If there are regions of charged domain walls in ferroelectric ceramic, it can enhance the extrinsic contribution to the piezoelectric and dielectric properties. We have performed a theoretical analysis on charged domain walls based on the time dependent Landau-Ginzburg model, assuming there are charge defects from aliovalent doping to locally stabilize such charged domain walls. Using $BaTiO_3$ and PZT as examples, we have studied the stability of charged walls with defect density and found that piezoelectric properties can be greatly enhanced by charged walls if the charge density ρ is lower than the charges needed to produce local charge balance. If the charge density is equal or more than the amount needed for electrical balance, the walls are pinned, which causes the reduction of piezoelectric effects. © *2012 American Institute of Physics*. [doi:10.1063/1.3679084]

I. INTRODUCTION

Understanding domain and domain wall properties is critical in the study of functional properties of ferroelectric materials, because it has been determined experimentally that ~70% of the dielectric and piezoelectric contributions in some ferroelectric materials can be attributed to domain related activities.[1,2] Extended Landau-Ginzburg theory is very powerful in describing domain structures and domain walls. Because its expansion coefficients can be directly determined from macroscopically measurable quantities, it can be used to quantitatively describe domain wall properties.[3,4] By adding a relaxation time evolution process, the model becomes the so called time dependent Ginzburg-Landau (TDGL) model, which can simulate domain evolution process from a quenched high temperature state and also demonstrate possible 2-D and 3-D domain patterns in ferroelectric systems.[5–8] In all previous studied situations, domain walls are all charge neutral walls because charged domain walls will be eliminated during the energy minimization process.

There is a long standing question about the mechanism of extrinsic contributions in PZT ceramics. With only 2%–3% Nb^{5+} doping, the piezoelectric properties can be doubled. The general hand waving argument is that the charged defects would interact with domain walls to produce much enhanced extrinsic contributions. However, how such small amounts of charged defects mobilize domain walls in the whole body is still physically unclear.

It was found using electron holography that charged defects, i.e., oxygen vacancies aggregate in 90° domain walls in $BaTiO_3$.[9] Therefore, it is possible that the presence of charged defects will stabilize in some ceramic grains or in regions inside the ceramic grains charged domain walls. When there is aliovalent doping, for example, either a 2^+ or a 5^+ ion to replace the 4^+ ion at the B-site of the ABX_3 perovskite structure, there will be localized charge imbalance. Such charge imbalance can be compensated through A-site or X site vacancies. This created many positive and negative charged defects in the system. Because charged defects could move under internal inhomogeneous field, particularly under the polarization gradient near the domains walls, they could stabilize charged domain walls. From energy consideration, the positive and negative charge defects will bond to the negatively or positively charged domain walls, respectively. When total charge balance is achieved, the charge defects provide pinning to the domain wall motions. In most cases, charge balance may not be complete at local sites so that the charged walls become less stable and will respond to external stimuli more vigorously to produce much enhanced extrinsic contributions.

It is possible to introduce dipolar defects into the model, and it was shown that these defects can greatly affect the coercive field.[10] One can also simulate the piezoelectric properties in a multidomain system and it was found that smaller domain size will produce larger extrinsic contributions to piezoelectric effects because domain walls make the system more responsive to external field.[11] Therefore, it is expected that charged domain walls will make the system even more responsive to external stimuli due to their less stable nature.

Based on the theoretical calculated energies of charged domain walls in ferroelectric crystals, it was concluded that charged domain walls could exist.[12] It was demonstrated that 180° head to head (HH) and tail to tail (TT) domain walls may be stabilized by intentional inserting the Sc^{3+} and Nb^{5+} to substitute some Ti^{4+}, respectively, in $PbTiO_3$ through first-principles calculations.[13] In general, 180° domain walls form

a)Electronic mail: dzk@psu.edu.

to minimize the electrostatic energy, while the experimentally observed 90° domains showed that the effect of elastic strain plays a major role in determining the domain morphology in ferroelectric materials. In the literature, most previous studies were concentrated on head to tail domain configuration, HH or TT 90° domain walls have never been studied using phenomenological theory, although such domains have been observed experimentally.[9,14] The aim of present work is to see how much defect charges are needed to stabilize the HH and TT 90° domains by incorporating the screened depolarization field and to simulate the changes of functional properties induced by the presence of such charged domain walls. As examples, we will use $BaTiO_3$ and PZT as model systems to demonstrate the effects of charged walls and to discuss related physical phenomena.

II. MODEL

The 3D Ginzburg-Landau free energy for ferroelectric systems has been given in Ref. 3. If the dimension along the domain wall is considered infinite, the system may be treated ad 2-dimensional. In such 2-D system, the square to rectangle transition is analogous to the cubic to tetragonal phase transition in 3D.

The total free energy for the 2-D system is given by

$$F = F_{local} + F_{gradient} + F_{electromechanical} + F_{electrostatic} + F_{charge} + F_{ext}. \quad (1)$$

The term F_{local} is the local free-energy given by

$$F_{local} = \int d\vec{r}\left\{\alpha_1\left(P_x^2 + P_y^2\right) + \alpha_{11}\left(P_x^4 + P_y^4\right) + \alpha_{12}P_x^2P_y^2 + \alpha_{111}\left(P_x^6 + P_y^6\right) + \alpha_{112}\left(P_x^2P_y^4 + P_x^4P_y^2\right)\right\}. \quad (2)$$

Here, P_x and P_y are the polarization components along x and y directions. The coefficients α_1, α_{11}, α_{111}, α_{12}, and α_{112} can be obtained from experimental data, which are related to linear and nonlinear dielectric permittivities.

$F_{gradient}$ is the polarization gradient energy,

$$F_{gradient} = \int d\vec{r}\left\{\frac{g_1}{2}\left(P_{x,x}^2 + P_{y,y}^2\right) + \frac{g_2}{2}\left(P_{x,y}^2 + P_{y,x}^2\right) + g_3P_{x,x}P_{y,y}\right\}, \quad (3)$$

where g_1, g_2, and g_3 can be measured from the phonon dispersion curve of the soft mode or from directly fitting the domain wall energies.[4,15]

$F_{electromechanical}$ is the electromechanical coupling energy, which can be written in the k-space considering the long range nature,

$$F_{electromechanical} = \lambda\int d\vec{k}\left|C_2\left(\vec{k}\right)\Gamma_2\left(\vec{k}\right) + C_3\left(\vec{k}\right)\Gamma_3\left(\vec{k}\right) - \Gamma_1\left(\vec{k}\right)\right|^2. \quad (4)$$

The above equation is obtained by eliminating the strains from the elastic free energy, subject to the elastic compatibility relations.[16] Here, $\Gamma_1(\vec{k})$, $\Gamma_2(\vec{k})$, and $\Gamma_3(\vec{k})$ are, respectively, the Fourier transforms of $Q_1(P_x^2 + P_y^2)$, $Q_2(P_x^2 - P_y^2)$, and $Q_3P_xP_y$;Q_1,Q_2, and Q_3 are calculated from the electrostrictive constants: $Q_1 = Q_{11} + Q_{12}$, $Q_2 = Q_{11} - Q_{12}$, and $Q_3 = Q_{44}$; $C_2 = (k_x^2 - k_y^2)/(k_x^2 + k_y^2)$ and $C_3 = k_xk_y/(k_x^2 + k_y^2)$ are orientation dependent.

$F_{electrostatic}$ is the electrostatic energy due to the screened depolarization field,

$$F_{electrostatic} = -\mu\int d\vec{r}\left\{\vec{E}_d\cdot\vec{P} + \varepsilon_0\left(\vec{E}_d\cdot\vec{E}_d/2\right)\right\}, \quad (5)$$

where $\vec{E}_d$ is the internal depolarization field and $\overrightarrow{E_d} = -\vec{\nabla}\phi$. When there are no free charges in the system, $\vec{\nabla}\cdot\left(\varepsilon_0\vec{E}_d + \vec{P}\right) = 0$.

The term F_{charge} represents the contribution to the free energy from the defect charges located in the TT or HH domain walls

$$F_{charge} = -\mu\int d\vec{r}\,\overrightarrow{E_{ch}}\cdot\vec{P}, \quad (6)$$

where $\overrightarrow{E_{ch}} = -\vec{\nabla}\phi_{ch}$, $\nabla^2\phi_{ch} = -\rho/\varepsilon_0$. In the above equation, ρ represents the additional positive or negative charge density put along the TT or HH domain wall, intending to stabilize charged domain walls.

The factor μ represent the interaction strength. It reflects the screening effect from the space charges. Because both depolarization field produced by the bond charges and the field from the defect charges will experience the same screening effect, μ appears in both Eqs. (5) and (6).

The term F_{ext} is given by

$$F_{ext} = -\int d\vec{r}\left(E_xP_x + E_yP_y\right), \quad (7)$$

E_x and E_y are the external electric field components applied in order to study the piezoelectric properties.

The dynamics of the polarization fields is governed by the relaxational master equation,

$$\frac{\partial P_i}{\partial t} = -\gamma\frac{\delta F}{\delta P_i}(i = x, y) \quad (8)$$

where γ is a dissipation coefficient and P_i represents the polarization components. For convenience of calculations,

TABLE I. Free energy coefficients we used for $BaTiO_3$.

Coefficients		Units
α_1	3.34×10^5 (T-381)	$Vm\,C^{-1}$
α_{11}	4.69×10^6 (T-393) -2.02×10^8	$Vm^5\,C^{-3}$
α_{111}	-5.52×10^7 (T-393) $+2.76\times10^9$	$Vm^9\,C^{-5}$
α_{12}	3.23×10^8	$Vm^5\,C^{-3}$
α_{112}	4.47×10^9	$Vm^9\,C^{-5}$
Q_{11}	0.11	$M^4\,C^{-2}$
Q_{12}	−0.045	$M^4\,C^{-2}$
Q_{44}	0.029	$M^4\,C^{-2}$
g	1.38×10^{-11}	$Vm^3\,C^{-1}$

TABLE II. Free energy coefficients we used for $Pb(Zr_{0.3}Ti_{0.7})O_3$.

Coefficients		Units
α_1	-1.2477×10^8	$Vm\ C^{-1}$
α_{11}	6.4579×10^6	$Vm^5\ C^{-3}$
α_{111}	2.3484×10^8	$Vm^9\ C^{-5}$
α_{12}	5.1093×10^8	$Vm^5\ C^{-3}$
α_{112}	1.025×10^9	$Vm^9\ C^{-5}$
Q_{11}	0.07887	$M^4\ C^{-2}$
Q_{12}	−0.0248	$M^4\ C^{-2}$
Q_{44}	0.06356	$M^4\ C^{-2}$
g	1.247×10^8	$Jm^3\ C^{-2}$

we introduce rescaled variables defined as the following: $u = P_x/P_0$, $v = P_y/P_0$, $\vec{r}^* = \vec{r}/\delta$, $\rho^*(\vec{r}^*) = \rho(\vec{r})/P_0$, and $t^* = \gamma|\alpha_1(T_0)|t$, where $T_0$is a fixed temperature. In this work we use $T_0 = 298$ K, $P_0 = 0.26$ Cm^{-2}, and $\delta = 0.5$ nm for $BaTiO_3$ and $T_0 = 298$ K, $P_0 = 0.647$ Cm^{-2} and $\delta = 1$ nm for $Pb(Zr_{0.3}Ti_{0.7})O_3$. The values for the long-range parameters are chosen as $\lambda = 0.25|\alpha_1(T_0)|/P_0^2$, $\mu = 40\varepsilon_0|\alpha_1(T_0)|$. For $BaTiO_3$, The free energy coefficients we used are listed in Table I taken from Ref. 17, the gradient coefficients are assumed $g_1 = g_2 = g_3 = g$ according to Ref. 11. For $Pb(Zr_{0.3}Ti_{0.7})O_3$, the free energy coefficients we used are listed in Table II taken from Ref. 18, and we assume the gradient coefficients $g_1 = g_2 = g$ and $g_3 = 0$ according to Ref. 19. We have checked other choices of these gradient coefficients and found that their influence to the effective piezoelectric coefficient is very small. This is because the gradient coefficients determine the stable structure of the domain wall, such as their thickness and energy, but the piezoelectric properties are related to the dynamic nature of the walls, which are determined by the stability of domain walls.

III. SIMULATIONS

In order to study domain pattern formation and related electromechanical properties, the TDGL equations are discretized using the Euler scheme on a 128×128 grid. Periodic boundary conditions are applied in both x^* and y^* directions. The space discretization steps are set as $\Delta x^* = \Delta y^* = 1$and the time interval is set as $\Delta t^* = 0.01$.

We simulated the properties of this 2-D model at $T = 298$ K. The initial conditions are chosen according to the following procedure.

Consider a function

$$R(x, y) = \cos\left(\frac{N\pi(x + y)}{128\delta}\right), \tag{9}$$

where the integer N represents the number of domain walls and the initial values are set by the following rules:

$$\begin{aligned} P_x(x, y) = P_0,\ P_y(x, y) = 0,\ \text{for } R(x, y) > 0, \\ P_x(x, y) = 0,\ P_y(x, y) = -P_0,\ \text{for } R(x, y) > 0. \end{aligned} \tag{10}$$

These initial conditions ensure that multidomain states with HH and TT domain walls oriented along [1 1] are formed as the starting point. The above initial conditions also ensure that only two of the four variants with HH and TT domain walls exist in the multidomain structure so that the system is polarized.

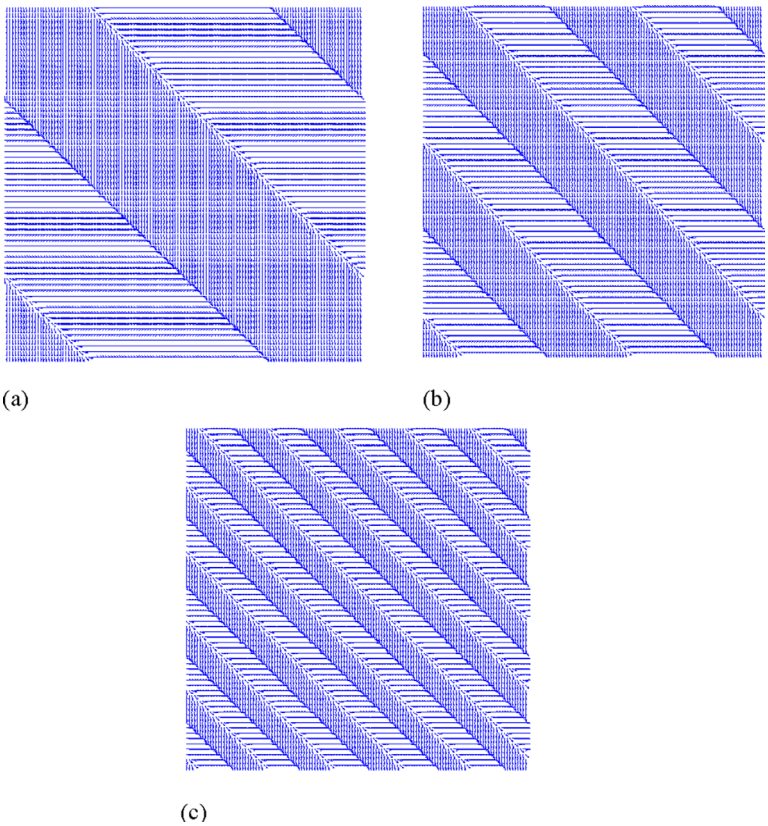

FIG. 1. (Color online) The HH and TT domain patterns with domain size (a) L ~ 22.6 nm, (b) L ~ 11.3 nm, and (c) L ~ 4.5 nm, respectively. The rescaled charge density ρ^* is chosen to be 1.9.

TABLE III. The variation of $d_{33}^{[10]}$ with the charge density ρ^* in the domain wall for $BaTiO_3$.

ρ^*	1.5	1.6	1.7	1.8	1.9	2.0
$d_{33}^{[10]}$(pC/N)	1104.1	527.4	334.2	244.5	165.9	85.8

For $BaTiO_3$, the length rescaling factor $\delta = 0.5$ nm, this discretization corresponds to a real system of 64 nm × 64 nm. In this simulation, we take a charge density ρ^* at each discretized grid in the domain wall to be a value from 1.5 to 2.0 in the increment of 0.1. We take $N = 2$, 4, and 10, corresponding to 90° domain patterns with mean domain sizes $L \sim 22.6$, 11.3, and 4.5 nm, respectively.

When the charge density ρ^* is equal to 1.9 ($\rho = 0.494$ cm^{-2} in real units) domain patterns with different N (domain wall number) are shown in Fig. 1. We can see that the HH and TT domain structures can be stabilized by these compensational negative or positive charges in the HH or TT domain walls. Therefore, this kind of charged domain walls can exist locally in ferroelectrics when there are sufficient charge defects in the system. In the relaxor-based single-crystal system $(1-x)Pb(Mg_{1/3}Nb_{2/3})O_3 - xPbTiO_3$ (PMN-PT), these charges may be provided by the ordering of Mg^{2+} or Nb^{5+}, because each unit cell can generate −2 or +1 extra-charges, respectively. Ordering of Mg^{2+} ions along the walls will generate HH domain walls while ordering of Nb^{5+} along the walls will stabilize TT domain configurations.

In order to investigate the electromechanical behavior, we applied an electric field along the [1 0] direction which is a polar direction. The field is applied quasi-statically, i.e., in small steps of $\Delta E_{[01]} = 0.092$ kV/cm, and we let the system relaxed for $t^* = 100$ time steps after each field increment. The piezoelectric coefficients are computed as the ratio of the strains over the applied electric field, for example, the piezoelectric coefficient $d_{33}^{[10]}$ is given by $d_{33}^{[10]} = \Delta\left(\langle \eta_{xx}(E_{[10]})\rangle\right)/\Delta E_{[10]}$. Here, $\eta_{xx}$is the strain component along [1 0] direction given by $\eta_{xx} = Q_{11}P_x^2 + Q_{12}P_y^2$. We used d_{33} to represent the piezoelectric coefficient along the poling direction in order to compare with the experimental values. As discussed above, our 2-D system has a direct correspondence with a 3-D system.

The calculated variation of $d_{33}^{[10]}$ with the local charge density in the domain walls for a system with 22.6 nm domain size is listed in Table III. From the table we can see that the $d_{33}^{[10]}$ increases drastically when charge density in the domain walls is decreased because the domain configuration become much less stable, which will result in more responsive to external field. On the other hand, excessive charges in the domain walls will pin the system so that the effective $d_{33}^{[10]}$ will become less compared to bulk properties.

TABLE IV. The change of $d_{33}^{[10]}$ with different domain size for $BaTiO_3$.

N	Domain size (nm)	$d_{33}^{[10]}$(pC/N)
2	22.6	165.9
4	11.3	195.9
10	4.5	249.1

TABLE V. The variation of $d_{33}^{[10]}$ with the charge density ρ^* in the domain wall for $Pb(Zr_{0.3}Ti_{0.7})O_3$.

ρ^*	1.2	1.3	1.4	1.5	1.6
$d_{33}^{[10]}$(pC/N)	1339.3	406.3	232.9	167.0	131.1

The calculated $d_{33}^{[10]}$ with the head to tail domain configuration is 145 pC/N. In comparison, we can conclude that the $d_{33}^{[10]}$ with HH and TT domain configuration is larger than that of head to tail domain configuration when the charge density ρ^* is lower than 1.9. Due to charge imbalance, the piezoelectric coefficient is greatly enhanced for lower ρ^*. When the charge density $\rho^* = 1.5$, the piezoelectric coefficient $d_{33}^{[10]}$ reaches 1104.1 pC/N, which is about 8 times of the value for the head to tail domain configuration.

We have also studied the influence of the size of HH and TT domains to the piezoelectric properties. The computed $d_{33}^{[10]}$ with different domain size is shown in Table IV for the charge density of $\rho^* = 1.9$. One can see that $d_{33}^{[10]}$ increases when the size of the HH and TT domains decreases. This is consistent with the experimental result of larger d_{33} for smaller domains.[20,21] Interestingly, if the charge density is sufficient to compensate the charged domain walls, piezoelectric effect becomes much smaller, which correspond to pinning effects.

As for $Pb(Zr_{0.3}Ti_{0.7})O_3$, we find that $d_{33}^{[10]}$ with the head to tail domain configuration is 192.9 pC/N. Based on the stable domain configuration requirement, the charge density ρ^* at each discretized grid in the domain wall is taken from 1.2 to 1.6 in the increment of 0.1. The calculated variation of $d_{33}^{[10]}$ with the local charge density in the two domain wall system is listed in Table V. We found that $d_{33}^{[10]}$ with HH and TT domain configuration is larger than that of head to tail domain configuration when the charge density ρ^* is lower than 1.4. When the charge density $\rho^* = 1.2$, the piezoelectric coefficient $d_{33}^{[10]}$ reaches as high as 1339.3 pC/N, which is about 7 times of the value for the head to tail domain configuration. This may be the reason for the large piezoelectric properties increase in PZT with only very small amount of alivalent doping.

IV. SUMMARY AND CONCLUSIONS

In summary, domain patterns and electromechanical properties of $BaTiO_3$ and PZT with HH and TT 90° domain walls are simulated by including the free energy due to the interaction between charge and polarization in the TDGL model with the consideration of the screened depolarization field. Although the electrostatic constrains normally prevent the HH and TT domain walls to form in ferroelectric materials, such charged domain structures can be stabilized by putting certain additional positive or negative charges in the TT or HH domain walls. Our theoretical results based on a phenomenological model explained the experimental observed functional properties produced by charged domain walls. We show that the piezoelectric properties of $BaTiO_3$ and PZT with charged domain walls are enhanced compared to the head to tail domain configuration and this may be the reason why the piezoelectric properties of PZT ceramic can be

increased drastically by only a small amount of alivalent doping. Our results also show that the $d_{33}^{[10]}$ increases with the decrease of the domain size, which is consistent with the experimental results.

ACKNOWLEDGMENTS

This research was supported by the Harbin Institute of Technology under the postdoctoral scholarship.

[1]A. G. Luchaninov, A. V. Shil'nikov, L. A. Shuvolov, and I. Ju. Shipkova, Ferroelectrics **29**, 47 (1980).
[2]A. V. Turik and A. V. Chernobabov, Zh. Tekh. Fiz. **47**, 1944 (1977).
[3]W. Cao and L. E. Cross, Phys. Rev. B. **44**, 5 (1991).
[4]W. Cao, J. Phys. Soc. Jpn. **63**, 1156 (1994).
[5]S. Nambu and D. A. Sagala, Phys. Rev. B **50**, 5838 (1994).
[6]H. L. Hu and L. Q. Chen, J. Am. Ceram. Soc. **81**, 492 (1998).
[7]W. Cao, S. Tavener, and S. Xie, J. Appl. Phys. **86**, 5739 (1999).
[8]H. L. Hu and L. Q. Chen, Mater. Sci. Eng. A **238**, 182 (1997).
[9]X. Zhang and T. Hashimoto, Appl. Phys. Lett. **60**, 784 (1992).
[10]R. Ahluwalia and W. Cao, Phys. Rev. B **63**, 012103 (2001).
[11]R. Ahluwalia and W. Cao, Phys. Rev. B **72**, 014112 (2005).
[12]Y. Y. Liu, J. J. Liu, S. H. Xie, and J. Y. Li, Appl. Phys. Lett. **91**, 172910 (2007).
[13]X. Wu and D. Vanderbilt, Phys. Rev. B **73**, 020103(R) (2006).
[14]J. H. Yin and W. Cao, J. Appl. Phys. **87**, 7438 (2000).
[15]J. Hilinka, Phys. Rev. B **74**, 104104 (2006).
[16]E. A. H. Love, *A Treatise on the Mathematical Theory of Elasticity* (Dover, New York, 1944).
[17]A. J. Bell, J. Appl. Phys. **89**, 3907 (2001).
[18]M. J. Haun, Z. Q. Zhuang, E. Furman, S. J. Jang, and L. E. Cross, Ferroelectrics **99**, 45 (1989).
[19]N. Ng, R. Ahluwalia, H. B. Su, and F. Boey, Acta Mater. **57**, 2047 (2009).
[20]S. Wada and T. Tsurumi, Br. Ceram. Trans. **103**, 93 (2004).
[21]Y. Xiang, R. Zhang, and W. Cao, J. Appl. Phys. **106**, 064102 (2009).